

Penalized Logistic Regression Analysis for Genetic Association Studies of Binary Phenotypes

Running head: Penalized Logistic Regression Analysis

Ying Yu ^{*1}, Siyuan Chen ¹, Samantha J. Jones ³, Rawnak Hoque ³, Olga Vishnyakova ³, Angela Brooks-Wilson ^{2,3} and Brad McNeney¹

¹*Department of Statistics and Actuarial Science, Simon Fraser University, Burnaby, BC, Canada*

²*Department of Biomedical Physiology and Kinesiology, Simon Fraser University, Burnaby, BC, Canada*

³*Canada's Michael Smith Genome Sciences Centre, Vancouver, BC, Canada*

Correspondence*:

Ying Yu
Statistics and Actuarial Science
Simon Fraser University
Burnaby, BC
V5A 1S6
Canada
+1-604-715-0217
ying.yu_5@sfu.ca

Keywords: Rare genetic variants, Penalized logistic regression, log-*F* priors, Monte Carlo EM, Laplace approximation, Data augmentation

Yu et al.

2 ABSTRACT

3 Introduction

4 Increasingly, logistic regression methods for genetic association studies of binary phenotypes
5 must be able to accommodate data sparsity, which arises from unbalanced case-control ratios
6 and/or rare genetic variants. Sparseness leads to maximum likelihood estimators (MLEs) of
7 log-OR parameters that are biased away from their null value of zero and tests with inflated type
8 1 errors. Different penalized-likelihood methods have been developed to mitigate sparse-data
9 bias. We study penalized logistic regression using a class of log- F priors indexed by a shrinkage
10 parameter m to shrink the biased MLE towards zero.

11 Methods

12 We propose a two-step approach to the analysis of a genetic association study: first, a set of
13 variants that show evidence of association with the trait is used to estimate m ; and second, the
14 estimated m is used for log- F -penalized logistic regression analyses of all variants using data
15 augmentation with standard software. Our estimate of m is the maximizer of a marginal likelihood
16 obtained by integrating the latent log-ORs out of the joint distribution of the parameters and
17 observed data. We consider two approximate approaches to maximizing the marginal likelihood:
18 (i) a Monte Carlo EM algorithm (MCEM) and (ii) a Laplace approximation (LA) to each integral,
19 followed by derivative-free optimization of the approximation.

20 Results

21 We evaluate the statistical properties of our proposed two-step method and compared its
22 performance to other shrinkage methods by a simulation study. Our simulation studies suggest
23 that the proposed log- F -penalized approach has lower bias and mean squared error than other
24 methods considered. We also illustrate the approach on data from a study of genetic associations
25 with “super senior” cases and middle aged controls.

26 Discussion/Conclusion

27 We have proposed a method for single rare variant analysis with binary phenotypes by logistic
28 regression penalized by log- F priors. Our method has the advantage of being easily extended
29 to correct for confounding due to population structure and genetic relatedness through a data
30 augmentation approach.

1 INTRODUCTION

31 Standard likelihood-based inference of the association between a binary trait and genetic markers is
32 susceptible to sparse data bias [1] when the case-control ratio is unbalanced and/or the genetic variant is
33 rare. In particular, when data are sparse, hypothesis tests based on asymptotic distributions have inflated
34 type I error [2] and the maximum likelihood estimator of odds-ratios is biased away from zero [3].

35 The relevance of sparse data bias to genetic association analysis is highlighted by recent work on methods
36 for genome-wide, phenome-wide association studies (PheWAS) of large biobanks. Despite the potential of
37 multivariate methods that jointly analyze phenotypes (e.g., [4]), approaches for PheWAS of biobank-scale
38 data typically reduce the problem to inferences of association between single nucleotide variants (SNVs)
39 and traits, adjusted for population structure and relatedness among subjects *via* a linear mixed model
40 (LMM) [5, 2] or whole genome regression (WGR) [6]. For valid testing of associations between rare
41 binary phenotypes and/or SNVs, SAIGE [2], EPACTS [7] and REGENIE [6] implement an efficient
42 saddle-point approximation (SPA) to the distribution of the score statistic that yields correct p-values.

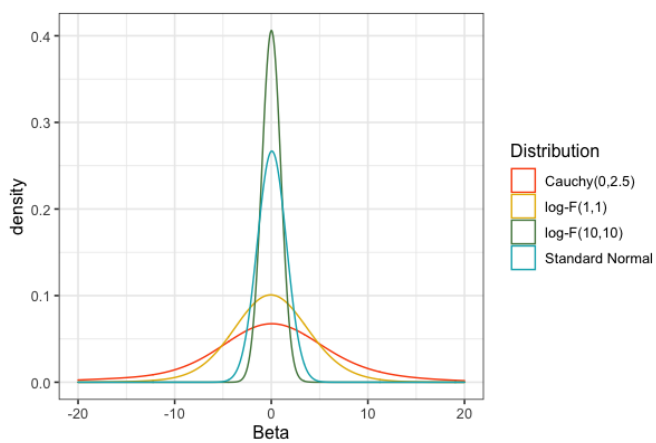


Figure 1. Comparison of log- F , standard normal and Cauchy distributions. The $\log-F(m, m)$ density is symmetrically bell-shaped with a single peak at zero, and its variance decreases as increasing m . As $m \rightarrow \infty$, the distribution tends toward a point mass at zero.

43 EPACTS and REGENIE also offer testing and effect estimation based on Firth logistic regression [3, 8],
44 a maximum-penalized likelihood method that uses the Jeffreys prior [9] as the penalty. In addition to
45 valid tests, the Firth logistic regression estimator of the odds-ratio is first-order unbiased. Reliable effect
46 estimates are important for designing replication studies and polygenic risk scores, and for fine-mapping
47 [10, section 2.3].

48 A variety of alternative penalties have been proposed for logistic regression, offering more or less shrinkage
49 than the Jeffreys prior [11]. Greenland and Mansournia developed penalized logistic regression based on a
50 class of log- F priors indexed by a shrinkage parameter m [12]. In our context, $\log-F(m, m)$ penalization
51 amounts to assuming that the log-OR parameter β for the SNV of interest has a $\log-F(m, m)$ distribution
52 with density

$$f(\beta|m) = \frac{1}{B(\frac{m}{2}, \frac{m}{2})} \frac{\exp(\frac{m}{2}\beta)}{(1 + \exp(\beta))^m}, \quad (1)$$

53 where $B(\cdot, \cdot)$ is the beta function (see Figure 1 for plots of $\log-F(1, 1)$ and $\log-F(10, 10)$ density curves).
54 In the $\log-F$ penalization approach, maximizing the posterior density is equivalent to maximizing a
55 penalized likelihood obtained by multiplying the logistic regression likelihood by the $\log-F(m, m)$ prior.
56 The explanatory variables of the logistic regression may include other covariates such as age, sex, genetic
57 principal components (PCs) or the predicted log-odds of being a case from a WGR. In general, we only
58 penalize the SNV of interest but do not penalize other confounding covariates or the intercept, as suggested
59 by Greenland and Mansournia [12].

60 Comparisons between $\log-F$ -penalized and Firth logistic regression are not straightforward because the
61 $\log-F$ approach penalizes selectively, while the Jeffreys prior used in Firth logistic regression is a function
62 of the Fisher information matrix for all coefficients, including the intercept. However, some insight can
63 be gained by comparing approaches for matched pairs data and a binary exposure. For matched pairs, the
64 standard analysis is conditional logistic regression, which eliminates intercept terms from the likelihood.
65 One can show that for a binary exposure Firth-penalized conditional logistic regression is equivalent
66 to imposing a $\log-F(1, 1)$ prior, which can be implemented by so-called Haldane correction [12]. For
67 Haldane correction we add 1/2 to each of the four cells in the 2×2 table of case/control \times exposure
68 status and perform a standard analysis of the augmented dataset. More generally, $\log-F(m, m)$ penalized

Yu et al.

69 analysis of matched pairs data is equivalent to analysis of the 2×2 table with each cell augmented by $m/2$
70 pseudo-individuals.

71 Limited simulation studies have shown that, for fixed m , $\log-F(m, m)$ penalized methods outperform other
72 approaches for case-control data [11]. Compared to Firth's method, the $\log-F$ approach is more flexible,
73 since we can change the amount of shrinkage by changing the value of m , and greater shrinkage may
74 reduce MSE [12]. However, there is little guidance on how best to select the value of m for a particular
75 phenotype. As a shrinkage parameter, m controls the bias-variance trade-off, with the variance of the
76 \log -OR estimator decreasing and the bias increasing as m increases [12]. We follow the suggestion by
77 Greenland and Mansourinia of using an empirical Bayes method to estimate m [12].

78 Our interest is in fitting single-SNV logistic regressions over a genomic region, or over the entire genome.
79 A motivating example is the Super Seniors study [13] that compared healthy "case" subjects aged 85 and
80 older across Canada who had never been diagnosed with cancer, dementia, diabetes, cardiovascular disease
81 or major lung disease to population-based middle-aged "controls" who were not selected based on health
82 status. The genetic data for this study are described in detail in Section 4. After quality control, data on
83 2,678,703 autosomal SNVs was available for 427 controls and 617 cases. A preliminary genome-wide scan
84 at a relatively liberal significance threshold of 5×10^{-5} found 57 SNVs associated with case-control status.

85 As in the Super Seniors data, the vast majority of SNVs have little or no effect, and a relatively small
86 set have non-zero effects. The prior used for penalization is the distribution of log-ORs for SNVs with
87 non-zero effects. We therefore propose to select K SNVs that show some evidence of having non-zero
88 effects in a preliminary scan, e.g., the $K = 57$ SNVs from the preliminary scan of the Super Seniors data,
89 and use these to estimate m . The intent is to learn about the distribution of non-zero log-ORs adaptively
90 from the data [14].

91 The main goal of this paper is to employ $\log-F$ penalized logistic regression for analyzing genetic variant
92 associations in a two-step approach. First, we estimate the shrinkage parameter m based on a set of
93 variants that show evidence of having non-zero effect in a preliminary scan. Second, we perform penalized
94 logistic regression for each variant in the study using $\log-F(m, m)$ penalization with m estimated from
95 step one. For a given m , the $\log-F$ penalized likelihood method can be conveniently implemented by
96 fitting a standard logistic regression to an augmented dataset [12]. In addition to estimates of SNV effects,
97 confidence intervals and likelihood ratio tests follow from the penalized likelihood [8]. Corrections for
98 multiple testing in GWAS/PheWAS applications would involve standard GWAS p-value thresholds, such
99 as 5×10^{-8} .

2 MODELS AND METHODS

100 We start by reviewing the penalized likelihood for cohort data, followed by the likelihood for case-
101 control data. We then introduce the penalized likelihood and derive a marginal likelihood for the shrinkage
102 parameter m based on data from a single SNV. Taking products of marginal likelihoods from K SNVs yields
103 a composite likelihood that we maximize to estimate m . We conclude by reviewing how $\log-F$ -penalized
104 logistic regression for the second-stage of the analysis can be implemented by data augmentation.

105 2.1 Likelihood from Cohort Data

106 Inference of associations between a single-nucleotide variant (SNV) and disease status from cohort data is
107 based on the conditional distribution of the binary response Y_i given the covariate X_i that encodes the SNV.
108 For a sample of n independent subjects let $\mathbf{Y} = (Y_1, \dots, Y_n)$ denote the vector of response variables and

Yu et al.

109 $\mathbf{X} = (X_1, \dots, X_n)$ denote the vector of genetic covariates. The likelihood is

$$L(\alpha, \beta) = P(\mathbf{Y}|\mathbf{X}, \alpha, \beta) = \prod_{i=1}^n \frac{\exp(Y_i(\alpha + X_i\beta))}{1 + \exp(\alpha + X_i\beta)}, \quad (2)$$

110 where α is an intercept term and β is the log-OR of interest.

111 2.2 Likelihood from Case-control Data

112 The association between a single-nucleotide variant (SNV) and disease status can also be estimated from
113 case-control (i.e. retrospective) data, in which covariates X_i are sampled conditional on disease status Y_i for
114 each individual i . Suppose there are n_0 controls indexed $i = 1, \dots, n_0$ and n_1 cases indexed $i = n_0 + 1, \dots, n$,
115 with $n = n_0 + n_1$ denoting the sample size of the study. Qin and Zhang [15] expressed the case-control
116 likelihood in terms of a two-sample semi-parametric model as follows

$$\begin{aligned} L(\beta, g) &= P(\mathbf{X}|\mathbf{Y}, \beta, g) = \prod_{i=1}^{n_0} P(X_i|Y_i = 0, g) \prod_{i=n_0+1}^{n_0+n_1} P(X_i|Y_i = 1, \beta, g) \\ &= \prod_{i=1}^{n_0} g(X_i) \prod_{i=n_0+1}^{n_0+n_1} c(\beta, g) \exp(X_i\beta) g(X_i), \end{aligned} \quad (3)$$

117 where $c(\beta, g)$ is a normalizing constant and $g(X)$ is the distribution of the covariates in controls, considered
118 to be a nuisance parameter. The potentially infinite-dimensional distribution g makes the case-control
119 likelihood $L(\beta, g)$ difficult to derive and maximize to find the MLE of β . Therefore, we rewrite the
120 case-control likelihood as a profile likelihood [16]:

$$\begin{aligned} L(\alpha^*, \beta) &= \prod_{i=1}^{n_0} \frac{1}{1 + \exp(\alpha^* + X_i\beta)} \prod_{i=n_0+1}^{n_0+n_1} \frac{\exp(\alpha^* + X_i\beta)}{1 + \exp(\alpha^* + X_i\beta)} \\ &= \prod_{i=1}^n \frac{\exp(Y_i(\alpha^* + X_i\beta))}{1 + \exp(\alpha^* + X_i\beta)}, \end{aligned} \quad (4)$$

121 where $\alpha^* = \alpha + \log\left(\frac{n_1}{n_0}\right) - \log\left(\frac{P(D=1)}{P(D=0)}\right)$, α is the intercept term in the logistic regression model for
122 $P(Y = 1|X)$, and $P(D = 1)$ and $P(D = 0)$ are the population probabilities of having and not having
123 the disease, respectively [17]. The profile likelihood $L(\alpha^*, \beta)$ for case-control data is of the same form
124 as the prospective likelihood. The MLE of β under the case-control sampling design can be obtained by
125 maximizing $L(\alpha^*, \beta)$ as if the data were collected in a prospective study [16, 15]. In what follows we write
126 the likelihood as in equation (4) with the understanding that $\alpha^* = \alpha$ for cohort data.

127 2.3 Penalized and Marginal Likelihoods

128 The penalized likelihood is obtained by multiplying the likelihood by a $\log-F(m, m)$ distribution (equation
129 (1)):

$$L_p(\alpha^*, \beta, m) = L(\alpha^*, \beta) f(\beta|m). \quad (5)$$

130 Integrating out the latent log-OR β gives a marginal likelihood of α and m :

$$L(\alpha^*, m) = \int L_p(\alpha^*, \beta, m) d\beta = \int L(\alpha^*, \beta) f(\beta|m) d\beta. \quad (6)$$

Yu et al.

131 In the above likelihood, the smoothing parameter m is the parameter of interest, while the intercept α^* is a
 132 nuisance parameter.

133 We expect very little information about m in data from a single marker, because this represents a single
 134 realization of β from the $\log-F(m, m)$ prior. In fact, empirical experiments (not shown) suggest a monotone,
 135 completely uninformative likelihood roughly 60-70 percent of the time. We therefore consider combining
 136 information across markers.

137 **2.4 Composite Likelihood for Estimating m with K markers**

138 Suppose there are K SNVs available for estimating m (see subsection 2.4.1). For each SNV we specify a
 139 one-covariate logistic regression model. Let \mathbf{X} denote a design matrix containing all K SNVs, and $\mathbf{X}_{\cdot k}$,
 140 $k = 1, \dots, K$, denote the genotype data on the k th SNV. Let $L_p(\alpha_k^*, \beta_k)$ denote the likelihood (4) for the
 141 k th log-OR parameter β_k . Here α_k^* is the intercept term from the k th likelihood, considered to be a nuisance
 142 parameter.

143 A composite likelihood [18, 19, 20] for $\alpha^* = (\alpha_1^*, \dots, \alpha_K^*)^T$ and m is the weighted product

$$L_{CL}(\alpha^*, m) = \prod_{k=1}^K L(\alpha_k^*, m)^{w_k}. \quad (7)$$

144 The corresponding composite log-likelihood is

$$l_{CL}(\alpha^*, m) = \sum_{k=1}^K w_k l(\alpha_k^*, m), \quad (8)$$

145 where $l(\alpha_k^*, m)$ is the marginal log-likelihood contribution from the k th variant obtained by integrating
 146 β_k out of the joint distribution of observed data and the parameter. Our estimate of m is the value
 147 that maximizes the composite log-likelihood equation (8). Following the notion that common variants
 148 should tend to have weaker effects and rare variants should tend to have stronger effects, we set
 149 $\sqrt{w_k} = 1/\sqrt{MAF_k(1 - MAF_k)}$ so that w_k is inversely proportional to the MAF of the k th SNV [21].
 150 The idea is to up-weight rarer variants of potentially greater effects and down-weight more common SNVs
 151 that may have smaller effects.

152

153 Maximization is done in two stages:

154 1. For fixed m , we maximize $l_{CL}(\alpha^*, m)$. The form of the composite likelihood when m is fixed, as a sum of
 155 terms involving only a single parameter, implies that to maximize $l_{CL}(\alpha^*, m)$ we maximize each $l(\alpha_k^*, m)$
 156 over α_k^* . Let $\hat{\alpha}_k^*(m)$ be the value of α_k^* that maximizes $l(\alpha_k^*, m)$, $\hat{\alpha}^*(m) = (\hat{\alpha}_1^*(m), \dots, \hat{\alpha}_K^*(m))$, and
 157 $l_{CL}(\hat{\alpha}^*(m), m) = \sum_{k=1}^K w_k l(\hat{\alpha}_k^*(m), m)$.

158 2. Maximize $l_{CL}(\hat{\alpha}^*(m), m)$ over m . To keep computations manageable, we restrict m to a grid of values,
 159 $m = 1, 2, \dots, M$. One may optionally smooth the resulting $(m, l_{CL}(\hat{\alpha}^*(m), m))$ pairs and maximize this
 160 smoothed curve to obtain the estimate \hat{m} .

161 For a fixed value of m and k , the estimate $\hat{\alpha}_k^*(m)$ can be obtained by maximizing $l(\alpha_k^*, m)$ with respect
 162 to α_k^* . However, it is difficult to evaluate the integral $\int L(\alpha_k^*, \beta_k) f(\beta_k|m) d\beta_k$ in (6). We discuss two
 163 approximate approaches. The first (Section 2.5.1) is a Monte Carlo EM algorithm [22], and the second

164 (Section 2.5.2) is a Laplace approximation to $L(\alpha_k^*, m)$ followed by derivative-free optimization of the
 165 approximation.

166 **2.4.1 Selecting variants for the composite likelihood**

167 Using variants with no effect in the composite likelihood leads to large estimates of m , which correspond
 168 to strong shrinkage toward zero. Over-shrinkage biases the log- F -penalized estimator towards zero, and
 169 reduces power in the second stage of analysis. In the extreme, the use of weakly-associated variants in the
 170 first stage can lead to a monotone marginal likelihood in m (results not shown). To avoid over-shrinkage
 171 we select SNVs with large marginal effects (i.e., small p-values) from a genome-wide scan, similar to
 172 the SNV-selection process used by FaST-LMM-Select [23]. For example, we can conduct a preliminary
 173 GWAS on all markers, or a thinned set of markers, and choose the SNVs with p-values below a multiple-
 174 testing-corrected threshold (refer this as Level 0 of Step 1). We then use the chosen SNVs to estimate m
 175 (Level 1 of Step 1).

176 **2.4.2 Adjustment for confounding variables and offsets**

177 We conclude this subsection by noting that it is possible to generalize the marginal likelihood approach
 178 for estimating m to incorporate non-genetic confounding variables, denoted Z , and known constants in
 179 the linear predictor, or "offset" terms, denoted b . As confounders, Z will be correlated with the SNV
 180 covariates X_k , and such correlation may differ across SNVs. We therefore introduce coefficients γ_k for
 181 the confounding variables in the logistic regression on the k th SNV. Offset terms can be used to include
 182 estimated polygenic effects in the logistic regression [6]. Expanding the α_k^* component of the logistic
 183 model to $\alpha_k^* + Z\gamma_k + b$, the k th likelihood is now

$$L(\alpha_k^*, \gamma_k, \beta_k) = \prod_{i=1}^n \frac{\exp(Y_i(\alpha_k^* + Z_i\gamma_k + b_i + X_{ik}\beta_k))}{1 + \exp(\alpha_k^* + Z_i\gamma_k + b_i + X_{ik}\beta_k)} \quad (9)$$

184 and the composite log-likelihood for estimating m is

$$\begin{aligned} l_{CL}(\boldsymbol{\alpha}^*, \boldsymbol{\gamma}, m) &= \sum_{k=1}^K w_k l(\alpha_k^*, \gamma_k, m) \\ &= \sum_{k=1}^K w_k \log \int L(\alpha_k^*, \gamma_k, \beta_k) f(\beta_k|m) d\beta_k. \end{aligned} \quad (10)$$

185 For fixed m we maximize $l_{CL}(\boldsymbol{\alpha}^*, \boldsymbol{\gamma}, m)$ by maximizing the component marginal likelihoods $l(\alpha_k^*, \gamma_k, m)$
 186 over the nuisance parameters (α_k^*, γ_k) . We then maximize the resulting expression over m to obtain \hat{m} .
 187 Though the generalization to include confounding variables and offsets is conceptually straightforward, we
 188 omit it in what follows to keep the notation as simple as possible.

189 **2.5 Maximization Approaches**

190 **2.5.1 Monte Carlo EM Algorithm**

191 To maximize $l(\alpha_k^*, m)$, we first consider an EM algorithm, which treats β_k as the unobserved latent variable
 192 or missing data. For a fixed value of m and k , the EM algorithm iterates between taking the conditional
 193 expectation of the complete-data log-likelihood given the observed data and the current parameter estimates,
 194 and maximizing this conditional expectation. The conditional distribution of β_k given the observed data is
 195 a posterior distribution that is proportional to the likelihood $L(\alpha_k^*, \beta_k)$ times the prior $f(\beta_k|m)$. Thus, at

Yu et al.

196 the $(p + 1)^{th}$ iteration, the E-step is to determine

$$Q \left(\alpha_k^* | \alpha_k^{*(p)}, m \right) \propto \int \log[L(\alpha_k^*, \beta_k) f(\beta_k | m)] L(\alpha_k^{*(p)}, \beta_k) f(\beta_k | m) d\beta_k \quad (11)$$

197 and the M-step is to set

$$\alpha_k^{*(p+1)} = \operatorname{argmax}_{\alpha_k^*} Q \left(\alpha_k^* | \alpha_k^{*(p)}, m \right). \quad (12)$$

198 The E-step (11) is complicated by the fact that the integral cannot be solved analytically. We therefore
199 approximate the integral numerically by Monte Carlo (MC); that is, we use a Monte Carlo EM (MCEM)
200 algorithm [24]. The MC integration in the E-step is obtained by sampling from the prior distribution
201 $f(\beta_k | m)$ [24, 25]. Based on a sample $\beta_{k1}, \dots, \beta_{kN}$ from the distribution $f(\beta_k | m)$, the MC approximation
202 to the integral is

$$\begin{aligned} Q \left(\alpha_k^* | \alpha_k^{*(p)}, m \right) &\approx Q_{MC} \left(\alpha_k^* | \alpha_k^{*(p)}, m \right) \\ &= \frac{1}{N} \sum_{j=1}^N \log[L(\alpha_k^*, \beta_{kj}) f(\beta_{kj} | m)] L(\alpha_k^{*(p)}, \beta_{kj}) \\ &= \frac{1}{N} \sum_{j=1}^N (\log[L(\alpha_k^*, \beta_{kj})] + \log[f(\beta_{kj} | m)]) L(\alpha_k^{*(p)}, \beta_{kj}). \end{aligned} \quad (13)$$

203 Note that $\log[f(\beta_{kj} | m)]$ is independent of the parameter α_k^* , so maximizing (13) in the M-step is equivalent
204 to maximizing

$$\frac{1}{N} \sum_{j=1}^N \log[L(\alpha_k^*, \beta_{kj})] L(\alpha_k^{*(p)}, \beta_{kj}). \quad (14)$$

205 For a discussion of computational approaches to the M-step see the online Supplementary Material.

206 2.5.2 Maximization of a Laplace Approximation

207 An alternative to the EM algorithm is to make an analytic approximation, $\tilde{L}(\alpha^*, m)$, to $L(\alpha^*, m) =$
208 $\int L(\alpha_k^*, \beta_k) f(\beta_k | m) d\beta_k$ and maximize this approximation. We considered Laplace approximation because
209 it is widely used for approximating marginal likelihoods [26]. The Laplace approximation of an integral is
210 the integral of an unnormalized Gaussian density matched to the integrand on its mode and curvature at the
211 mode. Letting $\hat{\beta}_k$ denote the mode of $L(\alpha_k^*, \beta_k) f(\beta_k | m)$ and $c_p(\alpha_k^*)$ minus its second derivative at $\hat{\beta}_k$, the
212 Laplace approximation to $L(\alpha_k^*, m)$ is

$$\tilde{L}(\alpha_k^*, m) = L(\alpha_k^*, \hat{\beta}_k) f(\hat{\beta}_k | m) \sqrt{\frac{2\pi}{c_p(\alpha_k^*)}}. \quad (15)$$

213 Each $\hat{\beta}_k$ is the root of the derivative equation $\partial \log(L(\alpha_k^*, \beta_k) f(\beta_k | m)) / \partial \beta_k = 0$; this can be shown to be a
214 global maximum of $L(\alpha_k^*, \beta_k) f(\beta_k | m)$. An expression for $c_p(\alpha_k^*)$ is given in Appendix A of [27]. Figure 2
215 shows the quality of the LA for one simulated dataset generated under $m = 4$. The approximate marginal
216 likelihood $\tilde{L}(\alpha_k^*, m)$ may be maximized over α^* using standard derivative-free optimization methods, such
217 as a golden section search or the Nelder-Mead algorithm.

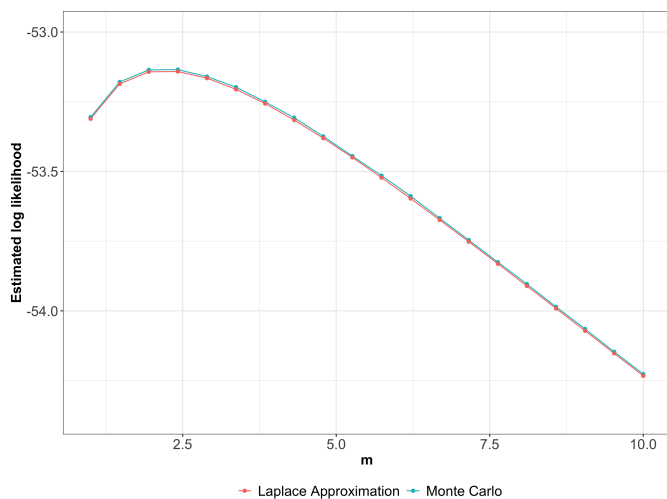


Figure 2. Natural logarithms of estimates of the marginal likelihood $L(\alpha_k^*, m)$ for one simulated dataset generated under $m = 4$. Estimates are obtained by LA and Monte Carlo. Log-likelihood estimates are plotted over the grid $m = (1, 1.5, \dots, 10)$ with $\alpha_k^* = -3$.

218 2.6 Implementing log-F Penalization by Data Augmentation

219 Penalization by a $\log-F(m, m)$ prior can be achieved by standard GLM through data augmentation
 220 suggested by Greenland and Mansournia [12]. Here, we provide some details. The logistic likelihood
 221 penalized by a $\log-F(m, m)$ prior (equation 5) is:

$$\begin{aligned}
 L_P(\alpha^*, \beta) &= \prod_{i=1}^n \frac{\exp(Y_i(\alpha^* + X_i\beta))}{1 + \exp(\alpha^* + X_i\beta)} \times \frac{\exp(\frac{m}{2}\beta)}{(1 + \exp(\beta))^m} \\
 &= \prod_{i=1}^n \frac{\exp(Y_i(\alpha^* + X_i\beta))}{1 + \exp(\alpha^* + X_i\beta)} \times \left[\frac{\exp(X_i\beta)}{1 + \exp(X_i\beta)} \right]^{\frac{m}{2}} \left[\frac{1}{1 + \exp(X_i\beta)} \right]^{\frac{m}{2}}, \tag{16}
 \end{aligned}$$

222 where $X_i = 1$. Thus, the penalized likelihood $L_p(\alpha^*, \beta)$ is equivalent to an unpenalized likelihood obtained
 223 by adding m pseudo-observations to the response with no intercept and covariate one, in which $m/2$ are
 224 successes and $m/2$ are failures (even if m is an odd number).

225 In our analyses (see Section 3), we analyze one SNV at a time using the $\log-F$ penalized logistic regression,
 226 adjusting for other confounding variables. The data augmentation approach is illustrated in Figure 3. Let X
 227 denote the allele count of a SNV and Z_j , $j = 1, \dots, p$, denote other confounding variables for adjustment.
 228 In the augmented dataset, the response is a two-column matrix with the number of successes and failures
 229 as the two columns. The m pseudo-observations are split into $m/2$ successes and $m/2$ failures. We only
 230 penalize the coefficient associated with the SNV, so we add a single row to the design matrix consisting of
 231 all zeros except for a one indicating the SNV covariate. Analyzing the augmented dataset with standard
 232 logistic regression yields the penalized MLE and its standard errors, as well as penalized likelihood ratio
 233 tests and penalized-likelihood-ratio-based confidence intervals. We conclude by noting that, for fixed m ,
 234 the influence of the m pseudo-observations on the fitted logistic regression diminishes as the sample size
 235 increases. In other words, for any m , the extent of penalization decreases with sample size.

		Response							
		Success	Failure	Intercept	X	Z_1	Z_2	\dots	Z_p
Original Dataset	1	0		1	0	x_{11}	x_{21}	\dots	x_{p1}
	0	1		1	2	x_{12}	x_{22}	\dots	x_{p2}
	\vdots	\vdots		\vdots	\vdots	\vdots	\vdots	\ddots	\vdots
Augmented Dataset	0	1		1	1	x_{1n}	x_{2n}	\dots	x_{pn}
	$m/2$	$m/2$		0	1	0	\dots	\dots	0

Figure 3. Illustration of data augmentation in the implementation of $\log-F(m, m)$ penalization.

3 A SIMULATION STUDY

236 The empirical performance of the methods introduced in Section 2 was evaluated in a simulation study.
 237 The proposed two-step $\log-F$ -penalized method (LogF) was compared with the standard MLE and the
 238 following methods:

239 •Firth logistic regression (FLR) was first proposed by Firth [3], where the logistic likelihood is penalized
 240 by $|I(\beta)|^{1/2}$ with $I(\beta) = -E\left[\frac{\partial^2}{\partial\beta^2}l(\beta)\right]$ defined as the Fisher information. FLR is implemented in the R
 241 function `logistf` of the package `logistf` [28].
 242 •Penalization by Cauchy priors (CP) was proposed by [29]. The input predictors are rescaled to have a
 243 mean of 0 and a standard deviation of 0.5. All predictors are penalized by a Cauchy prior with center 0
 244 and scale 2.5, whereas the intercept is penalized by a weaker Cauchy prior with center 0 and scale 10. CP
 245 is implemented in the R function `bayesglm` of the package `arm` [29].

246 All simulations were performed using R (Version 4.1.2) [30] on the Compute Canada cluster Cedar. We
 247 restricted m to a grid of values between 1 and 10, and we used parallel processing that splits the computation
 248 of the composite likelihood for each $m \in [1, 10]$ over different cores. Each node on the cluster has at least
 249 32 CPU cores and we allocated 10G to each core. For detailed description of its nodes' characteristics please
 250 refer to https://docs.computecanada.ca/wiki/Cedar#Node_characteristics.

251 We set the sample size to 500, 1000 and 1500, and 100 data sets were generated in each scenario. For each
 252 data set, we first estimated m based on a set of SNVs which show non-zero effects in a preliminary scan
 253 (Step 1), and then implemented the $\log-F$ penalized likelihood method to test single-variant association for
 254 each SNV by the data augmentation approach (Step 2). For the MLE and CP approaches we used Wald tests
 255 for SNV effects and Wald confidence intervals for the SNV coefficient. For FLR and the LogF approaches
 256 tests we used likelihood-ratio tests (LRTs). For a penalized log likelihood $l_P(\alpha, \beta)$, the likelihood ratio
 257 statistic [8] is

$$T = 2[l_P(\hat{\alpha}, \hat{\beta}) - l_P(\hat{\alpha}_0, 0)] \quad (17)$$

258 where $(\hat{\alpha}, \hat{\beta})$ is the maximum of the penalized likelihood function and $\hat{\alpha}_0$ is the maximum of the penalized
 259 likelihood when $\beta = 0$. The p-value is computed from the χ^2_1 distribution. For penalized logistic method,
 260 profile penalized likelihood (PPL) confidence intervals have shown to have better empirical properties than
 261 standard Wald-based confidence intervals [8]. A PPL confidence interval can be obtained by inverting the
 262 LRT, i.e., by finding all values of $\hat{\beta}_0$ such that $2[l_P(\hat{\alpha}, \hat{\beta}) - l_P(\hat{\alpha}_0, \hat{\beta}_0)] \leq \chi^2_{1,1-\alpha}$ gives a $100(1 - \alpha)\%$
 263 confidence interval for β .

264 **3.1 Data Generation**

265 To keep computations manageable, we simulate preliminary datasets of 50 causal and 950 null SNVs. Null
266 SNVs were used to assess the Type I error performance and the power was estimated using the set of causal
267 SNVs. The data was simulated according to a case-control sampling design, where covariates are simulated
268 based on disease status. For a given SNV, let X_j denote the allele count (i.e. 0, 1 or 2) of SNV $_j$ and β_j
269 be the corresponding log-OR parameter. Following [15], the conditional density function for X_j in the
270 controls and cases are

$$\begin{aligned} P(X_j = x|Y = 0) &= g(x) \text{ and} \\ P(X_j = x|Y = 1) &= h(x) = c(\beta_j, g) \exp(x\beta_j)g(x). \end{aligned} \tag{18}$$

271 We assume that the distribution of X in controls, $g(x)$, is Binomial(2, p), where p is the MAF of the SNV.
272 Then the distribution of X in cases, $h(x)$, is proportional to

$$g_z(x) \exp(x\beta_j) = \begin{cases} (1-p)^2 & x = 0 \\ 2p(1-p) \exp(\beta_j) & x = 1, \\ p^2 \exp(2\beta_j) & x = 2 \end{cases} \tag{19}$$

273 which has normalizing constant $(1-p)^2 + 2p(1-p) \exp(\beta_j) + p^2 \exp(2\beta_j)$.

274 We simulated data in the presence of population stratification. We create population-disease and population-
275 SNV associations as follows. To create population-disease association we introduced a population main
276 effect on disease risk by taking population-stratum log-OR, γ , to be 1. To create population-SNV association
277 we selected different SNV MAFs in different populations. Let Z denote a binary indicator of one of the two
278 population strata. The respective frequencies in controls of the two populations are f_0 and f_1 , respectively.
279 Then the distribution of Z in controls is $P(Z = z|Y = 0) = f_z$, and the distribution of Z in cases
280 is $P(Z = z|Y = 1) \propto f_z \exp(z\gamma)$ [31]. In our studies, we set $f_0 = f_1 = 0.5$. Now suppose that the
281 MAF for a given SNV differs by sub-population, with p_z denoting the MAF in population z . Let $g_z(x)$
282 denote the distribution of X_j in controls of population z , i.e., $P(X_j = x|Z = z, Y = 0) = g_z(x) \sim$
283 Binomial(2, p_z). The joint distribution of X and Z in controls is then $P(X_j = x, Z = z|Y = 0) = f_z g_z(x)$.
284 If $\text{logit}[P(Y = 1|Z = z, X_j = x)] = \alpha + z\gamma + x\beta_j$, the joint distribution of X and Z in cases is
285 $P(X_j = x, Z = z|Y = 1) \propto f_z g_z(x) \exp(z\gamma + x\beta_j)$ [15]. We then have

$$P(X_j = x|Z = z, Y = 1) = \frac{P(X_j = x, Z = z|Y = 1)}{P(Z = z|Y = 1)} \propto \frac{f_z g_z(x) \exp(z\gamma + x\beta_j)}{f_z \exp(z\gamma)} = g_z(x) \exp(x\beta_j). \tag{20}$$

286 To summarize, we first assigned population status for each subject using

$$\begin{aligned} P(Z = z|Y = 0) &= f_z, \\ P(Z = z|Y = 1) &\propto f_z \exp(z\gamma) = \begin{cases} f_0 & z = 0 \\ f_1 \exp(\gamma) & z = 1 \end{cases} \end{aligned} \tag{21}$$

287 Then using (19), we simulated the genotype data of each SNV_j , for $j = 1, \dots, 1000$, conditional on
288 population status by sampling from

$$P(X_j = x | Z = z, Y = 0) = g_z(x) \sim \text{Binomial}(2, p_z),$$
$$P(X_j = x | Z = z, Y = 1) \propto g_z(x) \exp(x\beta_j) = \begin{cases} (1 - p_z)^2 & x = 0 \\ 2p_z(1 - p_z) \exp(\beta_j) & x = 1 \\ p_z^2 \exp(2\beta_j) & x = 2 \end{cases} \quad (22)$$

289 MAFs, p_z , for different populations were obtained from 1000 Genomes Project [32]. Here we consider
290 two populations: Caucasian (CEU) and Yoruba (YRI) subjects, and we sampled MAFs of SNVs from a 1
291 million base-pair region on Chromosome 6 (SNVs with MAF = 0 have been removed). Data from the 1000
292 Genomes Project was downloaded using the Data Slicer (<https://www.internationalgenome.org/data-slicer/>). The effect sizes of causal SNVs were assumed to be a decreasing function of
293 MAF, which allows rare SNVs to have larger effect sizes and common SNVs to have smaller effect sizes.
294 We set the magnitude of each $\beta_j = \frac{\log 5}{2} |\log_{10} \text{MAF}_j|$ [21], where MAF_j is the pooled-MAFs $(p_0 + p_1)/2$
295 of the SNV_j . We took into account the effects of mixed signs, multiplying β_j by -1 for some j , in which
296 are 50% positive and 50% negative. This process gives the maximum OR = 6.44 ($|\beta_j| = 1.86$) for SNVs
297 with pooled-MAF = 0.0048 and the minimum OR = 1.40 ($|\beta_j| = 0.4$) for SNVs with pooled-MAF = 0.38
298 (Supplementary Figure 2 B).

300 3.2 Results

301 We first evaluated the performance of the two different log-F methods described above. Over 100 simulation
302 replicates, the mean estimates of m obtained by MCEM and LA are 4.77 (SD = 1.27) and 4.76 (SD = 1.18)
303 respectively for $n = 500$, and are 3.88 (SD = 1.56) and 3.83 (SD = 1.33) respectively for $n = 1000$. The
304 scatterplots (Figure 4) show good agreement between the two methods. Figure 5 compares the LA- and
305 MCEM-based likelihood curves of m for the first 20 simulated data sets. These likelihoods were plotted
306 with m of grid values from 1 to 10 on the x-axis, and each was smoothed by a smoothing spline. The
307 likelihood curves are of similar shape, though shifted because the MCEM approach estimates the likelihood
308 up to a constant (compare equations (13) and (14)). The compute time of LogF and FLR is given in Table
309 1. We see that LA is $160\times$ and $300\times$ faster than MCEM in elasped time for Step 1 when analyzing 1000
310 SNVs of sample size 500 and 1000, respectively. Although MCEM is computationally more expensive
311 than LA, the accuracy of its approximation can be controlled by the number of Monte Carlo replicates,
312 whereas the accuracy of LA cannot be controlled. We used $N = 1000$ Monte Carlo replicates in the MCEM
313 throughout, which gives reasonably good accuracy. The agreement of the MCEM and LA approaches for
314 smaller sample sizes validates the accuracy of LA. MCEM results are not available for the largest sample
315 size of $n = 1500$, because our current implementation fails due to numerical underflow. As expected, once
316 m is selected, LogF is computationally efficient as only a simple data augmentation approach is used in
317 Step 2. Combining Step 1 (with LA) and Step 2, along with the preliminary scan, which is of the same
318 order of computation time as Step 2, the combined computation time of the LogF approach is roughly half
319 that of FLR.

320 We further examined the accuracy of effect sizes from LogF-MCEM, LogF-LA, FLR and CP. All variants
321 were binned based on the pooled-MAF in five bins: (0%, 1%), [1%, 5%), [5%, 10%), [10%, 25%) and
322 [25%, 50%], and there were 51, 128, 213, 401, and 207 SNVs in each bin. The causal variants can be
323 either deleterious or protective (i.e. β_j is either positive or negative), so we define the bias of effect size
324 estimates as the signed bias, $E[\text{sign}(\beta_j)(\hat{\beta}_j - \beta_j)]$; positive values indicate bias away from zero, while

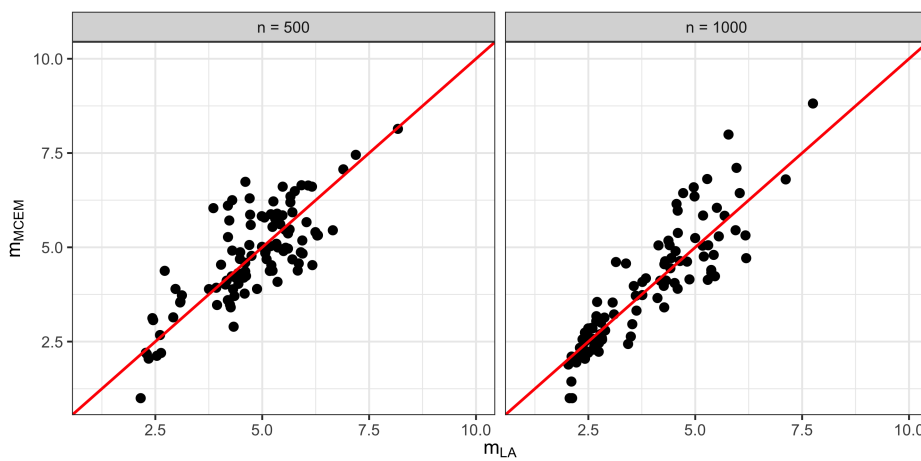


Figure 4. Scatterplot comparing the estimated values of m using the two methods over 100 simulation replicates. Values estimated by LA are on x-axis, and values estimated by MCEM are on y-axis. Red line is $y = x$.

325 negative values indicate bias towards zero. We also evaluated the SD of effect size estimates as the standard
326 deviation of $\hat{\beta}_j$ across 100 simulation replicates, and the mean squared error (MSE) as the sum of squared
327 bias and squared SD. MAF-binned results are shown in Table 2 and Figure 6. In the Figure, results for
328 the MLE obscure those for the other methods and are not shown. We find that for variants of MAF 1% or
329 greater, all methods are comparable. However, for rare variants of MAF < 1%, the SD of LogF is much
330 smaller than other methods. In addition, the signed bias of the LogF is more concentrated around zero
331 compared with other methods, though this tendency about zero is counteracted by some extreme negative
332 signed biases that suggest over-shrinkage in some cases. The MAFs of the three SNVs that lead to these
333 extreme negative signed biases (Figure 6) are 0.0048, 0.0072, and 0.0074, respectively. We note that 0.0048
334 was the smallest MAF in our simulated datasets. Combining bias and SD results in a much smaller MSE
335 for the LogF than other methods. Comparing the results under samples sizes of 500, 1000, and 1500, one
336 can see that penalization makes less of an impact as the sample size increases.

337 Through simulations, we also investigated the Type 1 error and power of the test of SNV effects from
338 the different approaches (Figure 7). Although all the methods provide good control of Type 1 error, we
339 found that LogF approaches result in a relatively smaller false positive rate. All the methods had similar
340 power, with slightly less power from LogF approaches. We believe that the increased power of the FLR
341 and Cauchy approaches can be partly attributed to their bias away from zero for rare variants.

4 DATA APPLICATION

342 The Super Seniors data from the Brooks-Wilson laboratory was collected to investigate the association
343 between genetic heritability and healthy aging of humans. The 'super seniors' are defined as those who are
344 85 or older and have no history of being diagnosed with the following 5 types of diseases: cardiovascular
345 disease, cancer, diabetes, major pulmonary disease or dementia. In this study, 1162 samples of 4,559,465
346 markers were genotyped using a custom Infinium Omni5Exome-4 v1.3 BeadChip (Illumina, San Diego,
347 California, USA) at the McGill University/Genome Quebec Innovation Centre (Montreal, Quebec, Canada)
348 [33]. The data underwent extensive quality control after genotyping, including re-clustering, removal of
349 replicate and tri-allelic SNPs, and checking for sex discrepancies and relatedness. We also removed SNPs
350 with MAF < 0.005, call rate < 97%, or Hardy-Weinberg equilibrium p-value < 1×10^{-6} among controls.

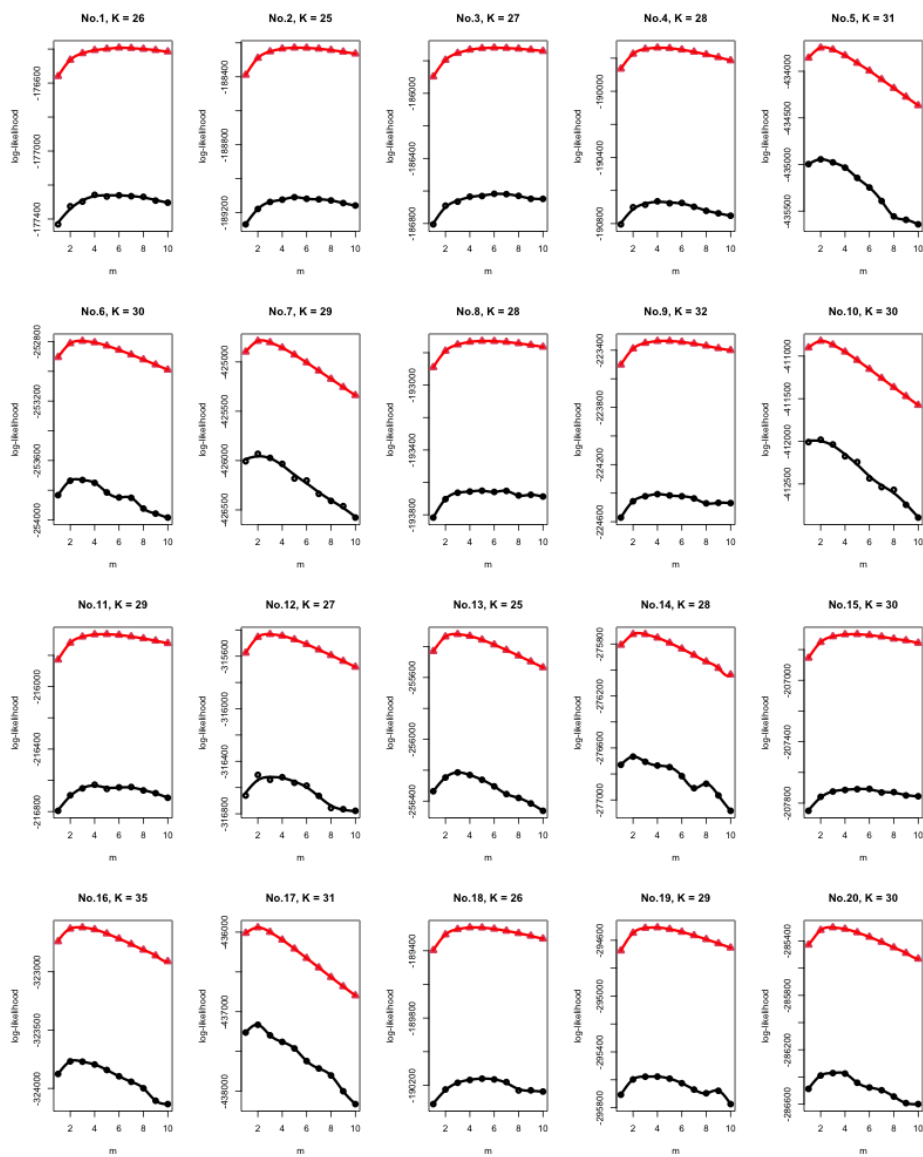


Figure 5. Comparison of profile log-likelihood curves obtained by the two different methods described in text, for the first 20 simulated data sets ($n = 1000$). In each case the likelihood curve was generated based on K SNVs selected in a preliminary genome-wide scan, and was smoothed by smoothing spline. The red line connecting triangles is based on LA, whereas the black line connecting dots corresponds to MCEM.

351 After a series of filtering steps, our final study includes 1044 self-reported Europeans, of which 427 are
 352 controls and 617 are cases (super seniors), and 2,678,703 autosomal SNPs.
 353 A preliminary genome-wide scan identified 98 SNPs with p -values $< 5 \times 10^{-5}$. Of these, the 57 SNPs with
 354 no missing values were used to estimate the value of m . Our marginal likelihood approach for estimating
 355 m incorporates sex and the first 10 principal components as confounding variables. The m estimated by
 356 MCEM and LA are 7.01 and 6.89, respectively. To analyse 2,678,703 SNPs, the LogF approach (Step 2)
 357 takes 14 hours, which is 30 \times faster than FLR (437 hours). Manhattan plots (Figure 8) show very good
 358 agreement for the association detected between methods. Figure 9 shows the QQ-plot of p -values when
 359 applying MLE, LogF-LA (results of LogF-MCEM are close to LogF-LA, and are shown in Supplementary
 360 Figure 5-8) and FLR to the Super Seniors data. All methods are close to the dashed line of slope one,

Method	Step	Min.	1st Qu.	Elapsed time (s)				
				Median	Mean	3rd Qu.	Max.	
<i>n</i> = 500								
LogF-MCEM	1	41	89	109	120	127	509	
LogF-LA	1	0.35	0.49	0.54	0.74	0.58	13.22	
LogF	2	3.53	3.66	3.69	3.78	3.92	4.31	
FLR	NA	10.48	10.94	11.09	11.18	11.36	12.36	
<i>n</i> = 1000								
LogF-MCEM	1	361	491	542	607	601	1274	
LogF-LA	1	1.02	1.51	1.68	1.79	1.82	3.73	
LogF	2	4.38	4.46	4.55	4.59	4.66	5.17	
FLR	NA	17.04	17.60	17.79	17.85	18.00	19.48	
<i>n</i> = 1500								
LogF-LA	1	2.42	2.66	2.75	2.78	2.89	3.73	
LogF	2	5.21	5.30	5.37	5.39	5.39	5.94	
FLR	NA	23.45	23.96	24.35	24.33	24.61	25.35	

Table 1. Computation time (elapsed time in seconds) of LogF and FLR when analyzing 1000 SNVs with sample size 500, 1000 and 1500 using 100 simulated data sets. No results are available for LogF-MCEM when *n* = 1500 due to numerical underflow.

361 though the FLR p-values veer up slightly above the line at $-\log_{10}$ p-values near 5. Figure 10 compares
 362 the parameter estimates of the MLE, FLR and LogF. Other than cases where the MLE appears grossly
 363 inflated (e.g., $|\hat{\beta}| > 5$), the estimates from the MLE and FLR are in surprisingly good agreement. The LogF
 364 estimates are shrunk more towards zero than those of FLR, and that the shrinkage is more pronounced for
 365 rare variants than for variants of frequency greater than 0.01. Figure 11 and Table 3 compare the p-values of
 366 the different approaches. The points below the dashed line of slope one in both panels of Figure 11 indicate
 367 that the FLR p-values are systematically lower than those of the MLE and LogF. This is also reflected in
 368 the confusion matrices of Table 3, which show that FLR flags more SNVs as significant at the 5×10^{-5}
 369 level than the other two methods. Taken together, these results suggest that the LogF approach may impose
 370 too much shrinkage on the SNV effect estimates.

5 DISCUSSION AND CONCLUSION

371 We have proposed a method for single rare variant analysis with binary phenotypes by logistic regression
 372 penalized by $\log\text{-}F$ priors. Our approach consists of two steps. First, we select K markers that show
 373 evidence of association with the phenotype in a preliminary scan and use these to estimate m . The value
 374 of m is the maximizer of a composite of K marginal likelihoods obtained by integrating the random
 375 effect out of the joint distribution of the observed data and the random effect. Our maximization algorithm
 376 contains two approximate approaches: (1) a hybrid of an EM algorithm and brute-force maximization of
 377 Monte Carlo estimates of the marginal likelihood; and (2) a combination of a Laplace approximation and
 378 derivative-free optimization of the marginal likelihood. The two methods give similar results, with LA
 379 being faster for all sample sizes and more numerically stable for large sample sizes. Second, $\log\text{-}F$ penalties
 380 are conveniently implemented with standard logistic regression by translating the coefficient penalty into a

Estimate	Method	MAF				
		(0%, 1%)	[1%, 5%)	[5%, 10%)	[10%, 25%)	[25%, 50%)
<i>n</i> = 500						
Bias ($\times 1000$)	MLE	69	-4	3	1	0
	CP	-8	-4	3	0	-0
	FLR	-6	-4	3	1	0
	LogF-MCEM	-41	-10	0	-0	-0
	LogF-LA	-40	-10	0	-0	-0
SD ($\times 1000$)	MLE	4832	487	267	187	147
	CP	909	405	263	184	145
	FLR	881	404	261	184	145
	LogF-MCEM	476	339	244	179	143
	LogF-LA	473	339	244	179	143
MSE ($\times 1000$)	MLE	27275	376	74	36	22
	CP	852	178	71	35	21
	FLR	799	177	71	35	22
	LogF-MCEM	259	122	62	33	21
	LogF-LA	256	122	62	33	21
Coverage* ($\times 1000$)	MLE	992	957	952	950	950
	CP	990	960	953	951	951
	FLR	967	951	950	950	950
	LogF-MCEM	983	965	958	952	952
	LogF-LA	984	965	958	952	952
<i>n</i> = 1000						
Bias ($\times 1000$)	MLE	51	4	-0	-0	-1
	CP	7	3	-1	-0	-1
	FLR	8	3	-1	-0	-1
	LogF-MCEM	-14	0	-2	-1	-1
	LogF-LA	-15	0	-2	-1	-1
SD ($\times 1000$)	MLE	1542	290	187	130	104
	CP	663	283	185	129	103
	FLR	661	282	185	129	103
	LogF-MCEM	491	263	180	128	103
	LogF-LA	489	263	180	128	103
MSE ($\times 1000$)	MLE	3590	92	36	17	11
	CP	462	87	36	17	11
	FLR	456	87	35	17	11
	LogF-MCEM	257	74	34	17	11
	LogF-LA	254	74	34	17	11
Coverage* ($\times 1000$)	MLE	976	953	951	951	946
	CP	974	954	951	952	946
	FLR	955	951	950	951	946
	LogF-MCEM	974	956	952	952	946
	LogF-LA	975	956	952	952	946
<i>n</i> = 1500						
Bias ($\times 1000$)	MLE	27	2	1	-0	-1
	CP	0	2	1	-0	-1
	FLR	-0	2	0	-0	-1
	LogF-LA	-11	0	-0	-0	-1
	MLE	782	236	151	106	83
SD ($\times 1000$)	CP	518	233	151	106	82
	FLR	522	232	150	106	83
	LogF-LA	447	225	149	105	82
	MLE	1060	61	24	12	7
	CP	279	59	23	12	7
MSE ($\times 1000$)	FLR	283	59	23	12	7
	LogF-LA	207	54	23	11	7
	MLE	968	949	950	950	952
	CP	971	951	951	950	953
	FLR	959	948	950	950	952
Coverage* ($\times 1000$)	LogF-LA	970	951	951	950	952

Table 2. MAF binned averages of bias, SD, MSE and CI coverage probability of effect size estimates across 100 simulated data. * Coverage probability of two-sided nominal 95% confidence intervals for log-OR coefficient. Wald CIs were used for MLE and CP, whereas profile likelihood-based CIs were used for FLR, LogF-MCEM and LogF-LA. No results are available for LogF-MCEM when *n* = 1500 due to numerical underflow.

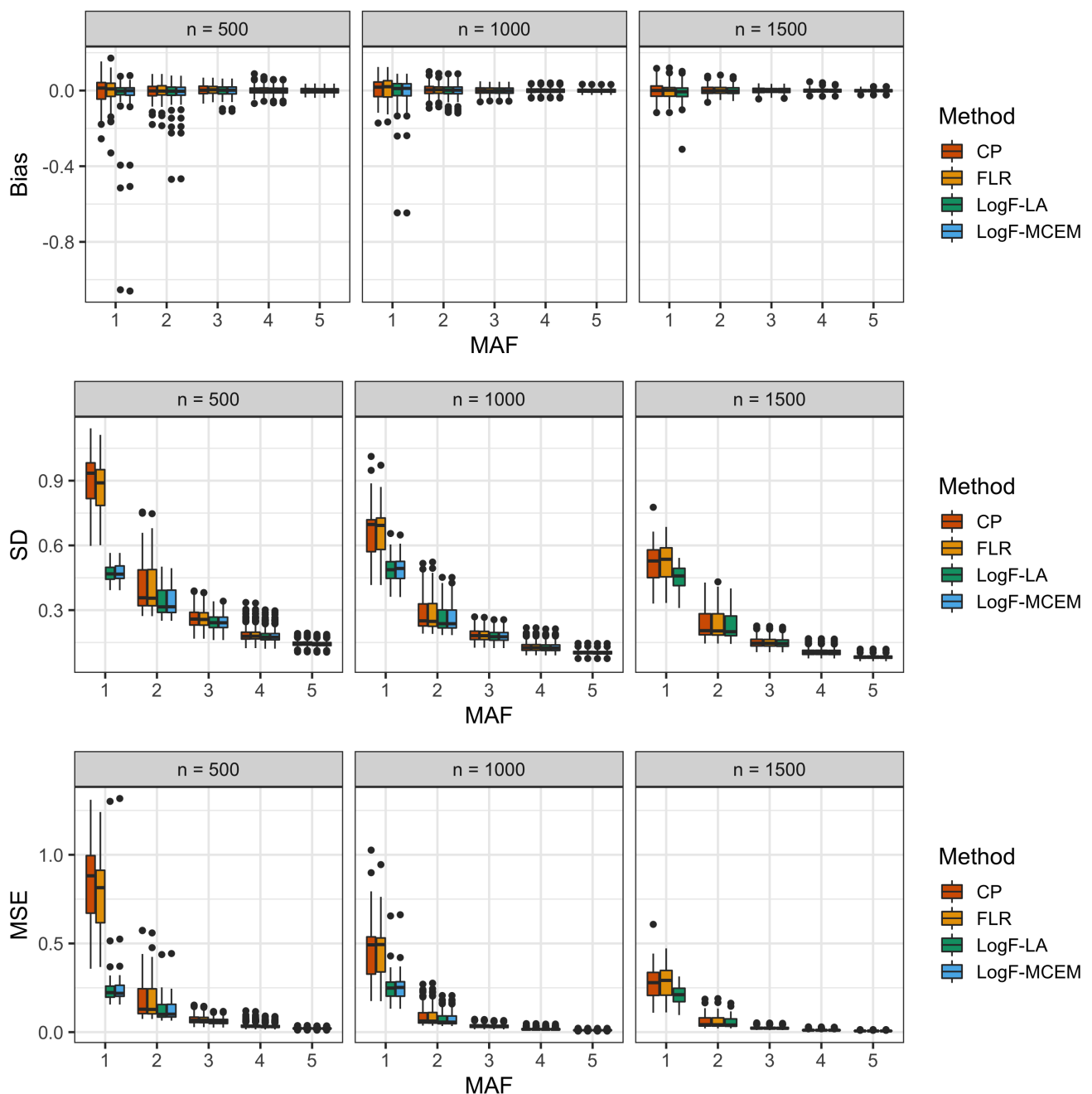


Figure 6. MAF binned boxplots of bias, SD and MSE of effect size estimates for LogF and other competing methods on simulated data. Each boxplot represents the distribution of the estimated quantity across 100 simulation replicates. MAF bins are: 1 = (0%, 1%), 2 = [1%, 5%), 3 = [5%, 10%), 4 = [10%, 25%) and 5 = [25%, 50%). No results are available for LogF-MCEM when $n = 1500$ due to numerical underflow.

381 pseudo-data record [12]. Our method requires extra computation time up front for the preliminary scan
 382 and selection of the shrinkage parameter m , but once selected, LogF approach (using LA in Step 1) is
 383 faster than Firth logistic regression (1). Our simulation studies suggest that the proposed LogF approach
 384 has slightly lower bias and substantially lower MSE than the other methods considered for variants of
 385 frequency less than 1%, and similar bias and MSE for variants of frequency greater than 1%. However, the
 386 power results of our simulation study and the analysis of the Super Seniors data suggest that our current

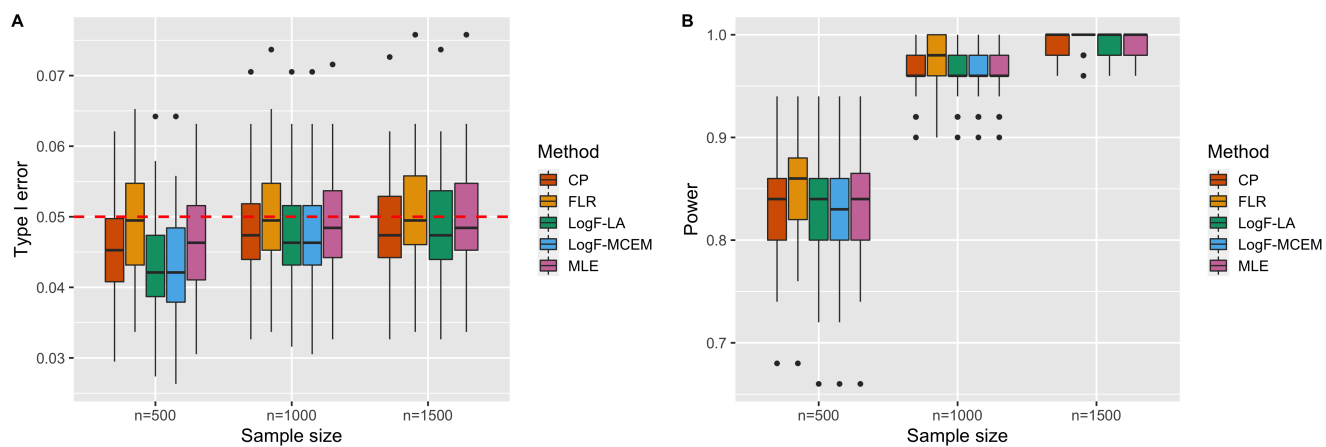


Figure 7. Type 1 error and power performance over simulated data sets. (A). Each boxplot represents the distribution of empirical type 1 error rates at nominal level 0.05 (red dashed horizontal line) across 100 simulation replicates computed at null SNVs. (B). Power computed at causal SNVs. No results are available for LogF-MCEM when $n = 1500$ due to numerical underflow.

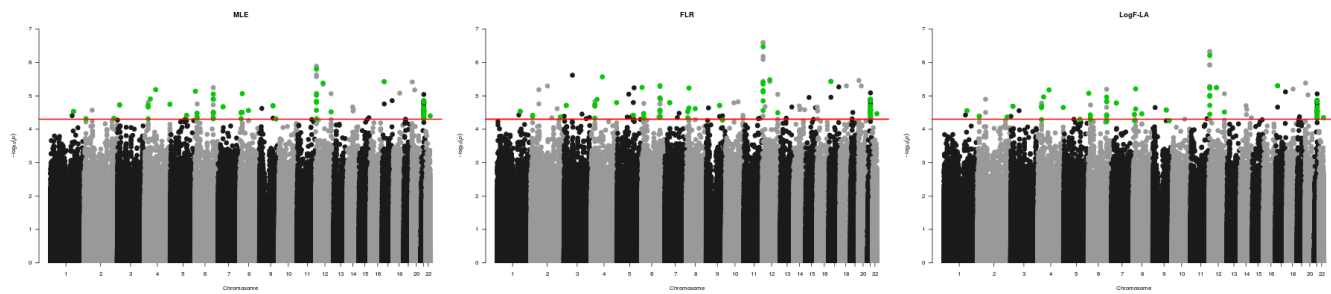


Figure 8. Manhattan plots comparing association results from different methods on Super Seniors data. The red horizontal line represents the liberal genome-wide significance threshold ($P = 5 \times 10^{-5}$) used to select SNPs in the preliminary scan. For LogF-LA, 57 SNPs (green points) below the threshold are used to estimate m in Step 1.

	MLE		LogF-LA		LogF-MCEM		
	0	1	0	1	0	1	
FLR	0	2678557	1	2678558	0	2678558	0
	1	42	97	45	94	46	93

Table 3. Confusion matrices comparing association results from different methods on Super Seniors data, where '1' indicating the number of SNPs below the genome-wide significant threshold of 5×10^{-5} and '0' otherwise.

387 implementation of log- F penalization has a tendency to over-shrink estimates of truly-associated SNVs.
 388 We discuss generalizations of the penalization approach that might correct such over-shrinkage in what
 389 follows.

390 Penalization can be generalized by allowing the prior distribution to depend on characteristics of the
 391 SNV, such as MAF or annotation information. A straightforward extension is to stratify selection of the
 392 shrinkage parameter by, e.g., MAF. That is, we might allow the prior distribution to be indexed by a
 393 variant-frequency-specific parameter instead of a common parameter for all variants. The idea could be

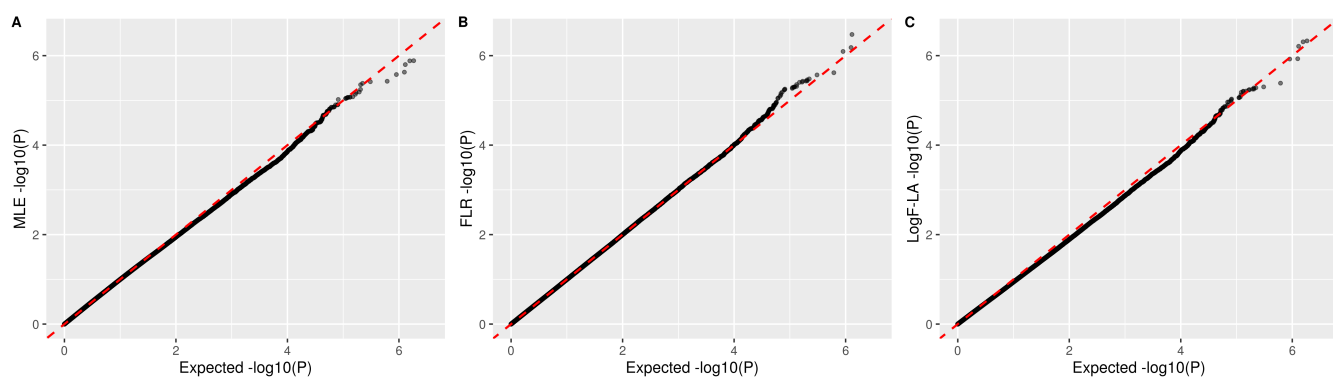


Figure 9. QQ-plot comparing p-values from different methods on Super Seniors data. The p-value for FLR and LogF-LA was obtained using the likelihood ratio test with a χ^2_1 test statistic.

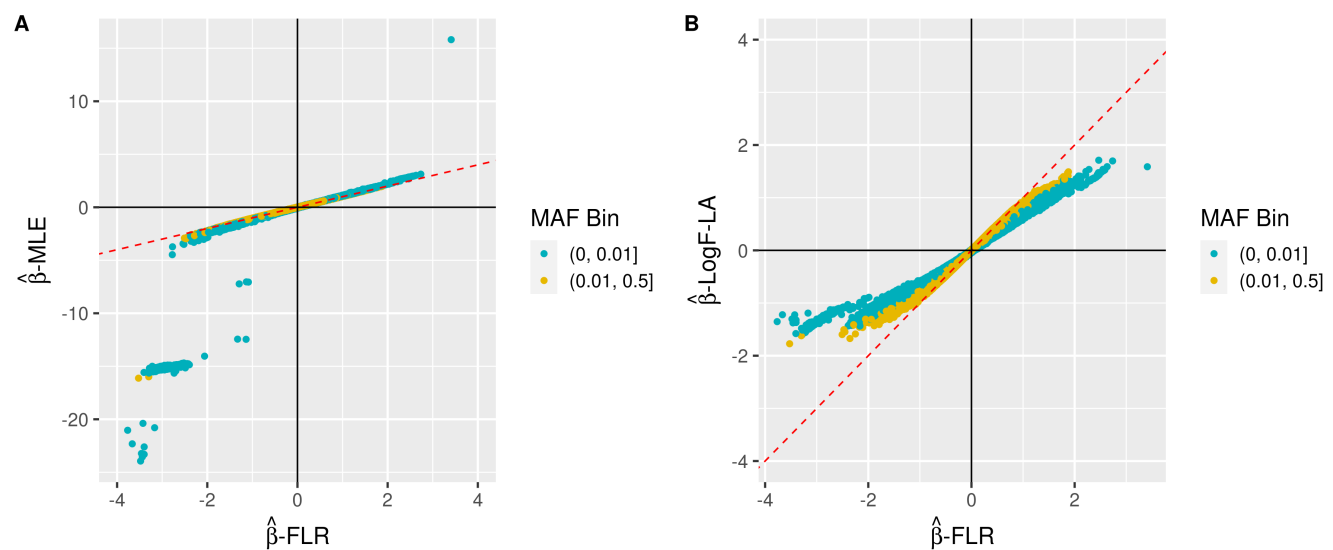


Figure 10. Scatterplots comparing effect size estimates from different methods for Super Seniors data. The plotting colors represents variant categories based on minor allele frequency (MAF) threshold of 1%.

394 as simple as multiplying the global shrinkage parameter m by a frequency-specific parameter α_k ; i.e., a
 395 variant in frequency bin k could have prior distribution $\log-F(\alpha_k m, \alpha_k m)$. We can choose the α_k values
 396 such that the distribution of common variants has a smaller variance and a larger variance for rare variants.
 397 In the context of heritability estimation [34] argue against stratified approaches and instead recommend
 398 modeling the variance of the SNV effects as proportional to $[f_i(1 - f_i)]^{1-\alpha}$ for MAF f_i and a power
 399 α . Their analyses of real data suggested the value $\alpha = -0.25$. This corresponds to standardizing each
 400 SNV covariate by dividing by $[f_i(1 - f_i)]^{(1-\alpha)/2}$ before analyses. In the context of modelling quantitative
 401 traits [35], proposing a double-exponential prior on SNV effects and a log-linear model for the scale
 402 parameter of the double exponential distribution allows the scale to depend on SNV characteristics such as
 403 annotation information. We plan to investigate the properties of both standardization and modelling of the
 404 shrinkage parameter on data from the UK Biobank. We also plan to use the UK Biobank data to investigate
 405 how the shrinkage parameter depends on phenotype characteristics such as prevalence and heritability.
 406 Application of the LogF approach to data from the UK Biobank will also confirm that the methods scale to
 407 biobank-sized datasets.

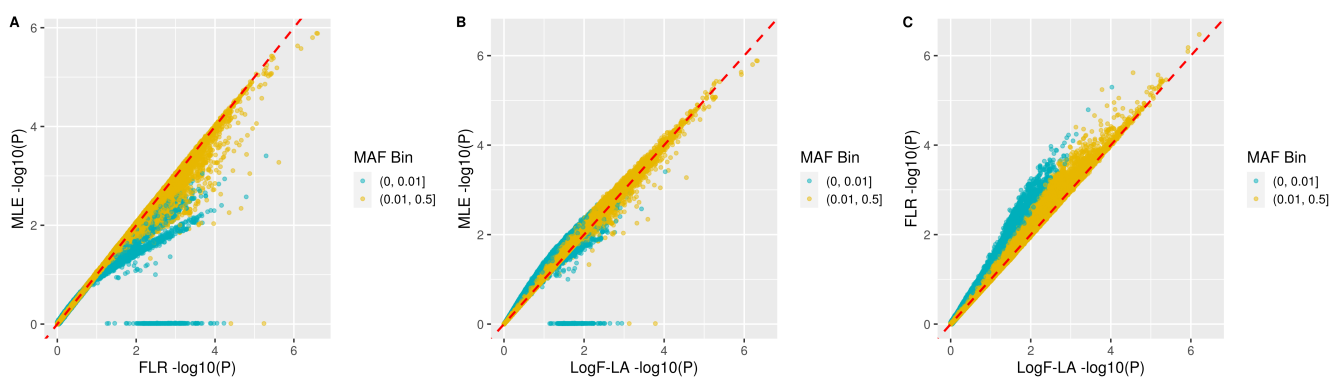


Figure 11. Scatterplots comparing p-values from different methods on Super Seniors data. The plotting colors represents variant categories based on minor allele frequency (MAF) threshold of 1%. For FLR and LogF-LA, the p-value for each variant was obtained by the likelihood ratio test with a χ^2_1 test statistic.

408 It should be noted that in our simulations we used a simplified, binary confounding variable to represent
409 population stratification. By contrast, the analysis of the Super Seniors data used an expanded set of
410 confounding variables that included sex and 10 principal components. We have also mentioned adjustment
411 for relatedness and population stratification by inclusion of an estimated polygenic effect as an "offset" in
412 the model. Another extension of interest is to use log- F penalization for a SNV covariate of interest in a
413 model that uses linear mixed models (LMMs) to correct for confounding due to population structure and
414 genetic relatedness [36, 37]. LMMs can be viewed as regression with correlated errors, using a kinship
415 matrix derived from anonymous SNVs to model correlations. It should be straightforward to extend this
416 regression approach to include log- F penalization of the SNV of interest through data augmentation.
417 Investigation of the properties of our approach in conjunction with LMMs is an area for future work.
418 In practice, identifying rare genetic causes of common diseases can improve diagnostic and treatment
419 strategies for patients as well as provide insights into disease etiology. Recent studies have found that
420 patients with low genetic risk scores (GRS) are more likely to carry rare pathogenic variants [38]. Although
421 GRS are currently based on common variants, our method might be of use in extending GRS methods to
422 include low-frequency or even rare variants of large effect sizes.
423 Our focus has been on single-SNV logistic regression, but log- F penalization generalizes to multiple-
424 variant logistic regression. In general, we multiply the likelihood by as many log- F distributions as there
425 are covariates whose coefficient we wish to penalize. This can also be implemented by a generalization of
426 the data augmentation procedure described in Section 2.6 [12, 39]. Such an approach may be useful for
427 performing the kinds of gene- or region-based tests that are commonly performed for rare variants, and
428 investigation of its properties is ongoing.

6 STATEMENTS

429 A preprint version of this article is available on bioRxiv [40].

430 6.1 Acknowledgment

431 The authors have no acknowledgment to declare.

432 6.2 Statement of Ethics

433 The Super Seniors study was approved by the joint Clinical Research Ethics board of BC Cancer and The
434 University of British Columbia. All participants provided written informed consent.

435 6.3 Conflict of Interest Statement

436 The authors have no conflicts of interest to declare.

437 6.4 Funding Sources

438 This work was supported, in part, by Discovery Grant RGPIN-05595 to Brad McNeney from the Natural
439 Sciences and Engineering Research Council of Canada (NSERC). The Super Seniors study was established
440 with a grant from the Canadian Institute of Health Research. Super Seniors genotype data generation
441 and preparation were supported by grants from the Lotte and John Hecht Memorial Foundation and the
442 Canadian Cancer Society.

443 6.5 Author Contributions

444 Ying Yu developed and implemented MCEM, generated simulated datasets, performed data application,
445 and drafted the manuscript. Siyuan Chen developed and implemented LA. Brad McNeney developed the
446 statistical methods and drafted the manuscript. Samantha J. Jones, Rawnak Hoque, Olga Vishnyakova, and
447 Angela Brooks-Wilson prepared and QC'd the Super Seniors data. All authors revised the manuscript and
448 approved the final version.

449 6.6 Data Availability Statement

450 Datasets simulated to evaluate the properties of the proposed method are available on request from the
451 corresponding author. R code to implement the methods is available from <https://github.com/SFUStatgen/logistlogF>.

REFERENCES

453 [1] Greenland S. Prior data for non-normal priors. *Stat Med* **26** (2007) 3578–3590.

454 [2] Zhou W, Nielsen JB, Fritsche LG, Dey R, Gabrielsen ME, Wolford BN, et al. Efficiently controlling
455 for case-control imbalance and sample relatedness in large-scale genetic association studies. *Nat
456 Genet* **50** (2018) 1335–1341.

457 [3] Firth D. Bias reduction of maximum likelihood estimates. *Biometrika* **80** (1993) 27–38.

458 [4] Zhou X, Stephens M. Efficient multivariate linear mixed model algorithms for genome-wide
459 association studies. *Nat Methods* **11** (2014) 407–409.

460 [5] Chen H, Wang C, Conomos MP, Stilp AM, Li Z, Sofer T, et al. Control for population structure and
461 relatedness for binary traits in genetic association studies via logistic mixed models. *Am J Hum Genet*
462 **98** (2016) 653–666.

463 [6] Mbatchou J, Barnard L, Backman J, Marcketta A, Kosmicki JA, Ziyatdinov A, et al. Computationally
464 efficient whole-genome regression for quantitative and binary traits. *Nat Genet* (2021) 1097–1103.

465 [7] Kang HM, Canouil M, Nguyen P. *EPACTS (Efficient and Parallelizable Association Container
466 Toolbox)* (2022).

467 [8] Heinze G, Schemper M. A solution to the problem of separation in logistic regression. *Stat Med* **21**
468 (2002) 2409–2419.

469 [9] Jeffreys H. An invariant form for the prior probability in estimation problems. *Proc R Soc Lon Ser-A*
470 **186** (1946) 453–461.

471 [10] Kraft P, Zeggini E, Ioannidis JPA. Replication in Genome-Wide Association Studies. *Stat Sci* **24**
472 (2009) 561 – 573.

473 [11] Graham J, McNeney B, Platt RW. Small sample methods. Breslow N, Borgan O, Chatterjee N, Gail
474 MH, Scott A, Wild CJ, editors, *Handbook of Statistical Methods for Case-Control Studies* (Boca Raton,
475 Florida: Chapman and Hall/CRC Press), Chapman & Hall/CRC Handbooks of Modern Statistical
476 Methods, chap. 9 (2018), 134–162.

477 [12] Greenland S, Mansournia MA. Penalization, bias reduction, and default priors in logistic and related
478 categorical and survival regressions. *Stat Med* **34** (2015) 3133–3143.

479 [13] Halaschek-Wiener J, Tindale LC, Collins JA, Leach S, McManus B, Madden K, et al. The Super-
480 Seniors Study: Phenotypic characterization of a healthy 85+ population. *PLoS One* **13** (2018)
481 e0197578.

482 [14] Zhou X, Carbonetto P, Stephens M. Polygenic modeling with bayesian sparse linear mixed models.
483 *PLoS Genet* **9** (2013) e1003264.

484 [15] Qin J, Zhang B. A goodness-of-fit test for logistic regression models based on case-control data.
485 *Biometrika* **84** (1997) 609–618.

486 [16] Prentice RL, Pyke R. Logistic disease incidence models and case-control studies. *Biometrika* **66**
487 (1979) 403–411.

488 [17] Scott AJ, Wild C. Maximum likelihood for generalised case-control studies. *J Stat Plan Infer* **96**
489 (2001) 3–27.

490 [18] Hudson RR. Two-locus sampling distributions and their application. *Genetics* **159** (2001) 1805–1817.

491 [19] Larriba F, Fearnhead P. On composite likelihood in statistical genetics. *Stat Sinica* **21** (2011) 43–69.

492 [20] Varin C, Reid N, Firth D. An overview of composite likelihood methods. *Stat Sinica* **21** (2011) 5–42.

493 [21] Wu MC, Lee S, Cai T, Li Y, Boehnke M, Lin X. Rare-variant association testing for sequencing data
494 with the sequence kernel association test. *Am J Hum Genet* **89** (2011) 82–93.

495 [22] Fahrmeir L, Tutz G. *Multivariate statistical modelling based on generalized linear models* (Springer
496 Science & Business Media) (2013).

497 [23] Listgarten J, Lippert C, Kadie CM, Davidson RI, Eskin E, Heckerman D. Improved linear mixed
498 models for genome-wide association studies. *Nat Methods* **9** (2012) 525–526.

499 [24] Wei GC, Tanner MA. A Monte Carlo implementation of the EM algorithm and the poor man's data
500 augmentation algorithms. *J Am Stat Assoc* **85** (1990) 699–704.

501 [25] Levine RA, Casella G. Implementations of the Monte Carlo EM algorithm. *Journal of Computational
502 and Graphical Statistics* **10** (2001) 422–439.

503 [26] Tierney L, Kadane JB. Accurate approximations for posterior moments and marginal densities. *J Am
504 Stat Assoc* **81** (1986) 82–86.

505 [27] Chen S. *Approximate Marginal Likelihoods for Shrinkage Parameter Estimation in Penalized Logistic
506 Regression Analysis of Case-Control Data*. Master's thesis, Simon Fraser University (2020).

507 [28] Heinze G, Ploner M, Dunkler D, Southworth H. logistf: Firth's bias reduced logistic regression. *R
508 package version 1* (2013).

509 [29] Gelman A, Jakulin A, Pittau MG, Su YS, et al. A weakly informative default prior distribution for
510 logistic and other regression models. *Ann Appl Stat* **2** (2008) 1360–1383.

511 [30] R Core Team. *R: A Language and Environment for Statistical Computing*. R Foundation for Statistical
512 Computing, Vienna, Austria (2020).

513 [31] Zhang B. Bias-corrected maximum semiparametric likelihood estimation under logistic regression
514 models based on case-control data. *J Stat Plan Infer* **136** (2006) 108–124.

515 [32] Consortium GP, et al. A global reference for human genetic variation. *Nature* **526** (2015) 68–74.

516 [33] Jones SJ. *Characterization of environmental and genetic factors in multiple-case lymphoid cancer*
517 *families*. Ph.D. thesis, University of British Columbia (2020). doi:<http://dx.doi.org/10.14288/1.0390430>.

518 [34] Speed D, Cai N, Johnson MR, Nejentsev S, Balding DJ. Reevaluation of SNP heritability in complex
519 human traits. *Nat Genet* **49** (2017) 986–992.

520 [35] Zeng C, Thomas DC, Lewinger JP. Incorporating prior knowledge into regularized regression.
521 *Bioinformatics* **37** (2021) 514–521.

522 [36] Kang HM, Sul JH, Service SK, Zaitlen NA, Kong Sy, Freimer NB, et al. Variance component model
523 to account for sample structure in genome-wide association studies. *Nat Genet* **42** (2010) 348–354.

524 [37] Lippert C, Listgarten J, Liu Y, Kadie CM, Davidson RI, Heckerman D. Fast linear mixed models for
525 genome-wide association studies. *Nat Methods* **8** (2011) 833–835.

526 [38] Lu T, Zhou S, Wu H, Forgetta V, Greenwood CM, Richards JB. Individuals with common diseases but
527 with a low polygenic risk score could be prioritized for rare variant screening. *Genetics in Medicine*
528 **23** (2021) 508–515.

529 [39] Yu Y. *Shrinkage parameter estimation for penalized logistic regression analysis of case-control data*.
530 Master's thesis, Simon Fraser University (2019).

531 [40] Yu Y, Chen S, McNeney B. Penalized logistic regression analysis for genetic association studies of
532 binary phenotypes (2021).

FIGURE LEGENDS

534 •Fig. 1. Comparison of log- F , standard normal and Cauchy distributions. The log- $F(m, m)$ density is
535 symmetrically bell-shaped with a single peak at zero, and its variance decreases as increasing m . As
536 $m \rightarrow \infty$, the distribution tends toward a point mass at zero.

537 •Fig. 2. Natural logarithms of estimates of the marginal likelihood $L(\alpha_k^*, m)$ for one simulated dataset
538 generated under $m = 4$. Estimates are obtained by LA and Monte Carlo. Log-likelihood estimates are
539 plotted over the grid $m = (1, 1.5, \dots, 10)$ with $\alpha_k^* = -3$.

540 •Fig. 3. Illustration of data augmentation in the implementation of log- $F(m, m)$ penalization.

541 •Fig. 4. Scatterplot comparing the estimated values of m using the two methods over 100 simulation
542 replicates. Values estimated by LA are on x-axis, and values estimated by MCEM are on y-axis. Red line
543 is $y = x$.

544 •Fig. 5. Comparison of profile log-likelihood curves obtained by the two different methods described in
545 text, for the first 20 simulated data sets ($n = 1000$). In each case the likelihood curve was generated
546 based on K SNVs selected in a preliminary genome-wide scan, and was smoothed by smoothing spline.
547 The red line connecting triangles is based on LA, whereas the black line connecting dots corresponds to
548 MCEM.

549 •Fig. 6. MAF binned boxplots of bias, SD and MSE of effect size estimates for LogF and other competing
550 methods on simulated data. Each boxplot represents the distribution of the estimated quantity across 100
551 simulation replicates. MAF bins are: 1 = (0%, 1%), 2 = [1%, 5%), 3 = [5%, 10%), 4 = [10%, 25%) and
552 5 = [25%, 50%). No results are available for LogF-MCEM when $n = 1500$ due to numerical underflow.

553 •Fig. 7. Type 1 error and power performance over simulated data sets. (A). Each boxplot represents the
554 distribution of empirical type 1 error rates at nominal level 0.05 (red dashed horizontal line) across

555 100 simulation replicates computed at null SNVs. (B). Power computed at causal SNVs. No results are
556 available for LogF-MCEM when $n = 1500$ due to numerical underflow.

557 •Fig. 8. Manhattan plots comparing association results from different methods on Super Seniors data. The
558 red horizontal line represents the liberal genome-wide significance threshold ($P = 5 \times 10^{-5}$) used to
559 select SNPs in the preliminary scan. For LogF-LA, 57 SNPs (green points) below the threshold are used
560 to estimate m in Step 1.

561 •Fig. 9. QQ-plot comparing p-values from different methods on Super Seniors data. The p-value for FLR
562 and LogF-LA was obtained using the likelihood ratio test with a χ^2_1 test statistic.

563 •Supplementary Fig. 1. $\mathbf{Y}_{(Nn \times 1)}$ is a vector containing N replicates of \mathbf{y} and $\mathbf{X}_{(Nn \times 1)}$ is a vector
564 containing N replicates of \mathbf{x} . \mathbf{W} stands for the weights for each Monte Carlo replicate such that
565 $W_j = f(\mathbf{X}_{\cdot k} | \alpha_k^{*(p)}, \beta_{kj})$ and the offset term $\mathbf{O} = \{\mathbf{x}\beta_{kj}\}_{j=1}^N$.

566 •Supplementary Fig. 2. A. Histogram of 1000 SNV-effect-sizes used for data simulation, in which
567 are 5 causal SNVs and 950 null SNVs. B. Histogram of effect sizes of causal SNPs, where $\beta_k =$
568 $\frac{\log 5}{2} |\log_{10} \text{MAF}_k|$.

569 •Supplementary Fig. 3. Effect sizes of 1000 SNVs generated used for data simulation by minor allele
570 frequency. Red dots indicate causal SNVs and blue dots indicate non-causal SNVs.

571 •Supplementary Fig. 4. Manhattan plots showing association results from LogF-MCEM on Super Seniors
572 data. The red horizontal line represents the liberal genome-wide significance threshold ($P = 5 \times 10^{-5}$)
573 used to select SNPs in the preliminary scan. 57 SNPs (green points) below the threshold are used to
574 estimate m in Step 1.

575 •Supplementary Fig. 5. QQ-plot showing p-values from LogF-MCEM on Super Seniors data. The p-value
576 was obtained using the likelihood ratio test with a χ^2_1 test statistic.

577 •Supplementary Fig. 6. Scatterplots showing effect size estimates from LogF-MCEM for Super Seniors
578 data. The plotting colors represents variant categories based on minor allele frequency (MAF) threshold
579 of 1%.

580 •Supplementary Fig. 7. Scatterplots comparing p-values from different methods on Super Seniors data.
581 The plotting colors represents variant categories based on minor allele frequency (MAF) threshold of 1%.
582 For FLR and LogF-MCEM, the p-value for each variant was obtained by the likelihood ratio test with a
583 χ^2_1 test statistic.

TABLE HEADINGS

584 •Table 1. Computation time (elapsed time in seconds) of LogF and FLR when analyzing 1000 SNVs with
585 sample size 500, 1000 and 1500 using 100 simulated data sets. No results are available for LogF-MCEM
586 when $n = 1500$ due to numerical underflow.

587 •Table 2. MAF binned averages of bias, SD, MSE and CI coverage probability of effect size estimates
588 across 100 simulated data. * Coverage probability of two-sided nominal 95% confidence intervals for
589 log-OR coefficient. Wald CIs were used for MLE and CP, whereas profile likelihood-based CIs were used
590 for FLR, LogF-MCEM and LogF-LA. No results are available for LogF-MCEM when $n = 1500$ due to
591 numerical underflow.

592 •Table 3.